Theor Chem Acc (2005) 114: 76–83
DOI 10.1007/s00214-005-0646-z

REGULAR ARTICLE

Gerrit Moritz · Markus Reiher · Bernd Artur Hess

Analysis of spin states, spin barriers, and *trans*-effects involved in the coordination and stabilization of dinitrogen by biomimetic iron complexes

Received: 15 October 2004 / Accepted: 20 November 2004 / Published online: 14 July 2005
© Springer-Verlag 2005

Abstract Coordination of dinitrogen to Sellmann-type iron (II) complexes in a sulfur-dominated coordination sphere, which emulates the environment of iron centers in the FeMo-cofactor of nitrogenase, is analyzed with respect to spin states, spin barriers, and the effect of *trans*-ligands. Such detailed investigations became only recently feasible when the reliability of density functional methods, which are the only quantum chemical methods capable of describing large transition metal complexes, could significantly be improved for the calculation of energies for states of different spin. It is found that the actual binding energy of dinitrogen is of sufficient magnitude for a reasonably strong fixation of N_2 by Sellmann-type coordination compounds. However, potential fixation is determined by additional factors which reduce the binding energy. One factor is the change in spin state of the N_2-free metal fragment, which lowers the total energy and quenches the thermodynamic stabilization effect of the binding energy. In addition, the metal fragment rearranges and gains even more stabilization energy for the un-coordinated state. Apart from these thermodynamical effects, the existence of spin barriers, which must be overcome upon binding of dinitrogen, leads to kinetical effects, which cannot be neglected.

1 Introduction

The catalytic reduction of dinitrogen to ammonia under ambient conditions with mild reductants, which is accomplished at the FeMo-cofactor (FeMoco) of the enzyme nitrogenase (see Ref. [1] for a recent collection of reviews on this subject), has not yet been achieved at iron centers of biomimetic model compounds though many attempts have been made (see, for instance, the extensive work by Sellmann et al. [2–5]). It was in 2003 when Yandulov and Schrock [6,7] synthesized the first catalytically active nitrogen-reducing complex, which is a mononuclear molybdenum species with a triamidoamine chelate ligand. Its potential role for understanding (and emulating) the mechanism of FeMoco is not crystal clear though [8]. The seven iron centers in FeMoco [9] cannot yet be ruled out as the potential catalytic site of FeMoco. Recent quantum chemical studies based on density functional theory (DFT) attribute a major role in the reduction process to these iron centers [10–13]. Since the FeMoco represents a huge challenge for any present-day DFT method because of complicated spin–spin interaction patterns and dense lying electronic states, the focus of our work was on biomimetic model compounds of the Sellmann type (see Ref. [14] for a review). Typically, these complexes are dinuclear with iron or ruthenium as metal centers. Their chelate ligand sphere consists of thiolate and thioether functionalities, which may serve as proton acceptors for the transfer of protons onto the dinitrogen species. In very recent work, we could demonstrate how to transfrom inert molecular nitrogen coordinated to Sellmann-type complexes into diazene — which is the most important reduction step — in a well-directed manner [15,16]. However, this hypothetical mechanism can only be tested experimentally if dinitrogen complexes with iron or ruthenium centers in sulfur ligand sphere can be synthesized — a goal, which has been achieved for a single ruthenium-based complex only recently [17–20].

Understanding dinitrogen coordination at biomimetic Sellmann-type complexes is thus the most important and most difficult step for these systems [21]. In order to gain insight into this reaction we utilize DFT calculations. Standard density functionals, however, do not yield reliable reaction energetics if states of different spin multiplicity get close [22–26]. We could show that the amount of exact exchange admixture in hybrid density functionals depends linearly on the exact exchange contribution and needs to be reduced (to 15% in the case of the B3LYP [27,28] functional) in order to obtain reliable spin state energetics for transition metal complexes in general [29,30] and for Sellmann-type complexes in particular [25].

In previous work, we studied the reduction energetics at mononuclear Sellmann-type complexes [21]. One result of

G. Moritz · M. Reiher (✉) · B.A. Hess
Institut für Physikalische Chemie, Universität Jena, Helmholtzweg 4, 07743 Jena, Germany
E-mail: markus.reiher@uni-jena.de

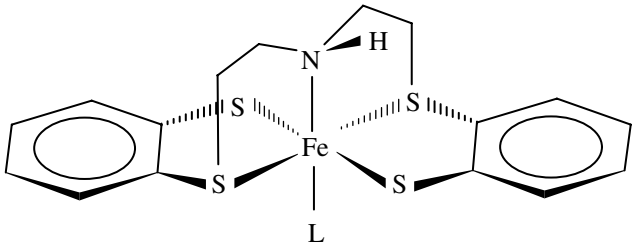

Fig. 1 Lewis structure of a Sellmann-type mononuclear biomimetic model complex **1**. This system is experimentally known with various ligands such as CO, NO^+ and phosphanes

this study was that the coordination energy of N_2 in such complexes must be increased in order to finally arrive at a biomimetic catalytic reduction process. This necessary increase in coordination strength was determined from a thermodynamical rather than a kinetical point of view; there are thus many potential reasons for this overall small coordination energy. In this study, we therefore investigate the coordination of dinitrogen in greater detail in order to aid experimental studies in their pursuit of finding stable dinitrogen iron complexes in sulfur ligand sphere. The main question to be answered is why it has not yet been possible to bind dinitrogen to such Fe(II)–sulfur complexes. One hint stems from results [21] that show a spin flip from low- to high-spin of the metal fragment upon dissociation of N_2, which leads to a significant decrease in energy such that the total coordination energy is negligibly small. Hence, we investigate the role of states of different spin, spin barriers, and the *trans*-ligand effects on the coordination mode of dinitrogen to mononuclear biomimetic Fe(II) complexes in this work. The importance of different spin states and intersystem crossing in the coordination chemistry of N_2 has also been observed and discussed by Tuczek and co-workers for iron in phosphane ligand sphere [31] and by Keogh and Poli for an organometallic molybdenum complex [32] although the high-spin state of the metal fragments in these cases were higher in energy so that coordination of N_2 was energetically favorable.

This work is organized as follows: In the next section details on the quantum chemical methodology are given. In Sect. 3, the Sellmann-type complex under consideration is introduced and Sect. 4 describes model complexes, which are needed for the investigation of the effect of different ligands in *trans*-position in order to grasp the role of high-spin states and spin barriers.

2 Quantum chemical methodology

From the computational point of view, large dinitrogen complexes of transition metals with a complicated system of low-lying electronic states are hardly accessible by present day ab initio quantum chemical methods. Only methods based on density functional theory are feasible for practical reasons.

For tests on internal consistency, we employed the Becke–Perdew functional BP86 [33,34] and a variant of the hybrid functional B3LYP [27,28], which is our B3LYP* functional [25,29,30]. The B3LYP* functional is a B3LYP with a reduced exact exchange contribution from 20% to 15%. The density functionals BP86 and B3LYP were chosen since they are the most well established representatives of pure and hybrid density functionals yielding reasonable reaction energetics in a large number of cases [35]. However, the situation is different for iron compounds where highly unreliable energetics were obtained for complexes of the type under consideration [26]. A systematic study has shown that these iron complexes represent critical cases where high-spin–low-spin energy splittings are small and differ largely when calculated with pure and hybrid density functionals [25]. In order to avoid these uncertainties we use for the discussion of energetics only the B3LYP* functional, which originated from studies on Sellmann-type complexes [25] but which turned out to be of general applicability [30].

For all calculations we employed the density functional programs provided by the TURBOMOLE 5.1 suite [36]. All results were obtained from all-electron calculations; restricted optimizations were carried out for singlet (low-spin) states, while all triplet (intermediate-spin) and quintet (high-spin) states as well as the singlet state in the potential energy curve calculations were treated in the spin-unrestricted framework. In connection with the BP86 functional, we always applied the resolution-of-the-identity (RI) technique [37,38]. Ahlrichs' TZVP basis set [39] featuring a valence triple-zeta basis set plus polarization functions on all atoms was used throughout. All minimum structures were fully optimized with the corresponding density functional and basis set. Frequency analyses have been carried out with our SNF program package [40], which calculates the Hessian matrix in a semi-numerical manner by finite-difference differentiation of analytic gradients at slightly distorted geometries. Partial charges have been calculated from modified atomic orbitals within a scheme for population analysis based on occupation numbers (PABOON) with multicenter corrections [41–43] as implemented in TURBOMOLE. The program MOLDEN [44] has been used for the visualization of structures.

In calculations of potential energy curves [45], we used the B3LYP* functional and relaxed all structural parameters of a complex in its singlet state except for the ligand–metal bond length, which was forced to assume a pre-defined value. Energies for all states of higher spin were obtained at these optimized singlet structures. Consequently, the potential energy curves of the higher spin states represent an upper bound to corresponding curves which would be obtained for relaxed structures of higher spin. Note, however, that structural relaxation of the vertically excited singlet structures in the high-spin (quintet) state would lead to dissociation of the dinitrogen ligand in the complexes under study: the high-spin states do not bind N_2.

For a sufficiently large number of test calculations on similar Fe(II)–sulfur complexes, we found [21] that reaction energies calculated with this TZVP and the even larger TZVPP (with additional polarization functions) basis sets differed by only ca. 5 kJ/mol without correcting for the basis-set

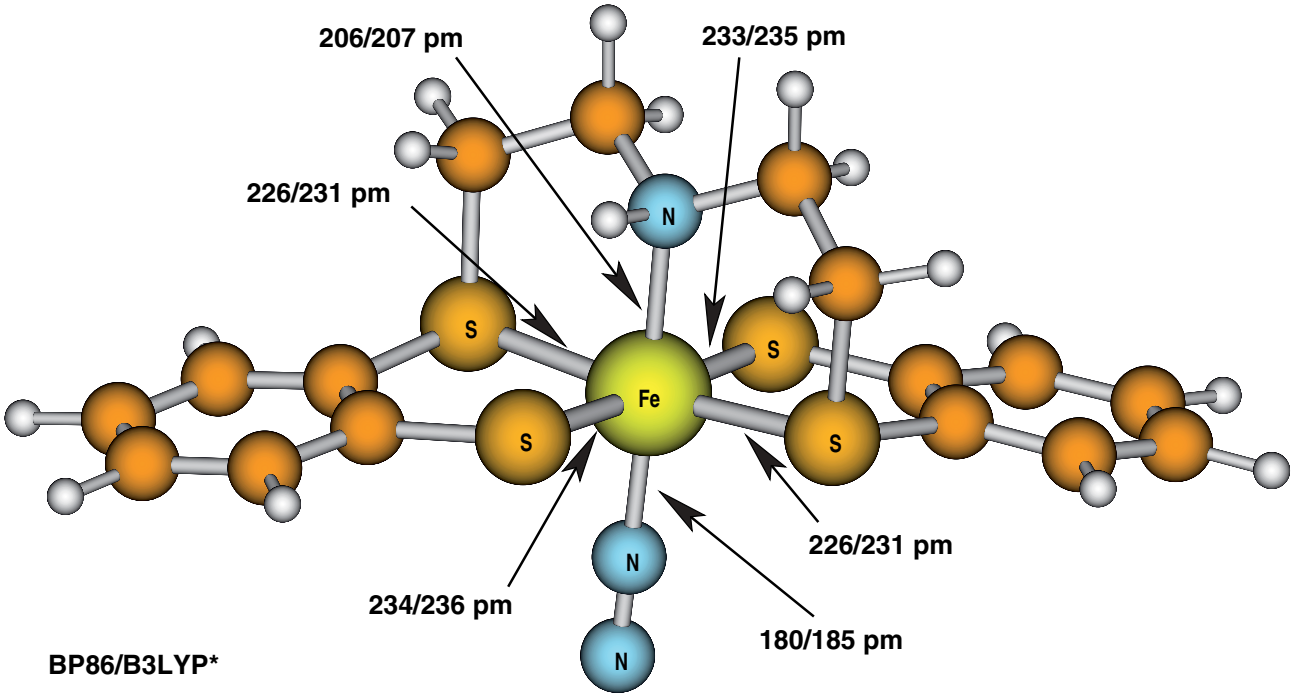

Fig. 2 Optimized structures of the Sellmann-type mononuclear compound **1** with N_2 as sixth ligand

superposition error (BSSE). If a counter-poise correction was added, our test calculations on coordination energies have shown that results obtained with the TZVP and the TZVPP basis sets differ by less than 1 kJ/mol. We were thus led to the conclusion that the TZVP basis set in combination with the counter-poise correction [46,47], which we included for all points on the potential energy curves presented in this paper, is sufficiently accurate for our purposes.

3 A Sellmann-type model complex

Sellmann and collaborators have developed an impressive chemistry of iron–sulfur complexes based on the assumption that the FeMoco of nitrogenase opens up on N_2 uptake and coordinates N_2 to (two) iron centers. The mononuclear iron complex **1** (depicted in Fig. 1) is one of the experimentally best characterized iron(II) complexes [3]. It is known with various ligands, e.g., L=CO, NO^+, or phosphane, but not with L=N_2. The diazene complex of this system has been obtained in dinuclear form [48,49].

Optimizing the structure of the experimentally not known hypothetical complex **1**(L=N_2) yields the structure depicted in Fig. 2 (the spin multiplicity is singlet). It is interesting to note that frequency analysis confirms the N_2 complex of **1** to be a minimum structure on the potential energy surface of the isolated system. This is remarkable because the potential energy surface can easily become repulsive with respect to coordination of N_2, if, for instance, the spin state of the ground state would be high- instead of low-spin (see below).

Since **1**(N_2) is stable in a quantum chemical sense (i.e., it represents a (local) minimum on the potential energy surface), the question arises, why has it not yet been possible to synthesize this complex. The reason for this may be anticipated in view of the results on a homologous complex [21], for which a change from low- to high-spin of the metal fragment leads to a significant decrease in energy such that the overall coordination energy is largely quenched. In order to analyze this mechanism in greater detail, we calculated the singlet-state potential energy curve for coordination of N_2 and the corresponding vertical excitation energies into the quintet state (B3LYP*/TZVP; see Fig. 3).

Figure 3 clearly shows that the coordination of N_2 on the singlet potential energy surface is indeed exothermic (by about −60 kJ/mol; see also Table 1) and leads to a stable minimum structure. We note in passing that the potential energy curve of intermediate spin (i.e., the triplet state) is found to lie between the high- and low-spin curves. The intermediate spin state is thus never the ground state and we restrict our discussion to the high- and low-spin states only. Vertical excitation into the repulsive potential energy surface of the quintet state requires about 140 kJ/mol at the singlet minimum structure but only about 30 kJ/mol in the asymptotic region. Relaxation of the high-spin metal fragment leads to a significant energy gain resulting from a trigonal-bipyramidal distortion, see Fig. 4. We should emphasize that N_2 cannot be bound to the quintet state, which we checked by structure optimization of the high-spin complex (this was also found for the model complexes to be discussed in the next section).

The structural rearrangement of the five-coordinate metal fragment and the associated energy gain are the reason why

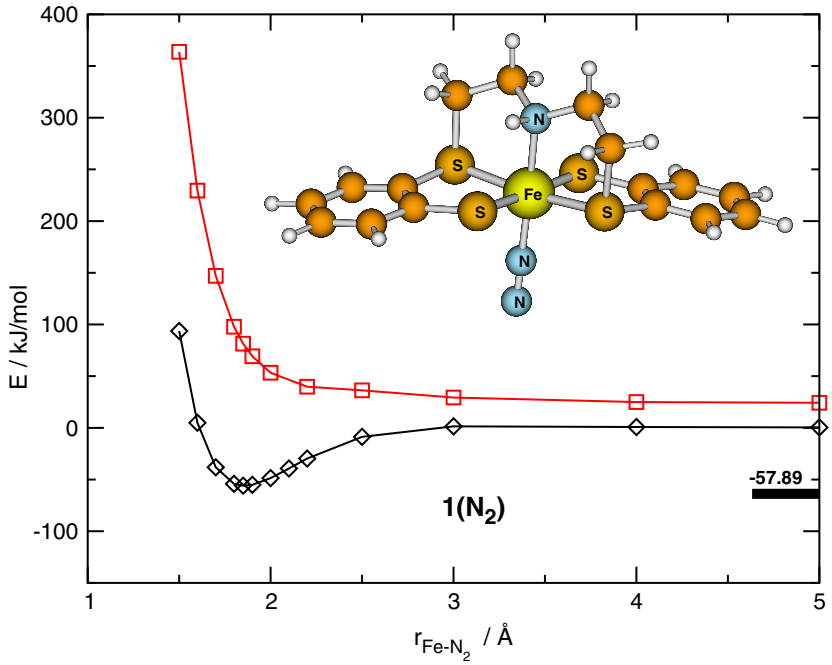

Fig. 3 Counter-poise corrected potential energy curves for the coordination of N_2 to the metal fragment of **1** (B3LYP*/TZVP). The (*red*) high-spin quintet curve was calculated at the partially relaxed singlet structures (*black curve*). The *bold bar* at the right-hand-side of the figure denotes the energetical position of the relaxed high-spin fragment. The energetic difference between this *bold bar* and the *red* asymptote corresponds to the energy, which is gained after structural relaxation of the high-spin state at the low-spin structure

the coordination of N_2 to iron centers in Sellmann-type ligand spheres is not favorable from a thermodynamical point of view. In turn, there arises a kinetical aspect since an inevitable crossing of different spin states must occur when N_2 is coordinated to the metal fragment. It is likely that this spin barrier is the reason why coordination of N_2 to five-coordinate Sellmann-type metal fragments has not yet been achieved experimentally because the spin barrier had to be overcome when the N_2 would be approaching the metal fragment in the asymptotic region. Note that the spin barrier incorporates two energetically unfavorable processes: (1) the spin flip is in general a forbidden process (if spin–orbit coupling is sufficiently small) and (2) the structural rearrangement of the metal fragment from trigonal-bipyramidal to square-pyramidal requires a significant amount of energy.

On the other hand, the spin barrier could protect an N_2 coordinated at the metal fragment. But in order to generate such a situation, it would be necessary to generate the **1**(N_2) complex from a more stable N_2H_x species, which has also not yet been achieved experimentally. One reason is that such an 'in situ' generation of the **1**(N_2) complex would be hindered by effective side reaction like those described in Ref. [16], which need to be suppressed. Consequently, the most obvious solution of this dilemma would be to prevent the distortion of the metal fragment in order to keep the singlet state as the ground state also in the asymptotic region. This might be achieved sterically through a particularly chosen chelate ligand architecture or electronically through the ligand field strength of the only non-sulfur ligand in *trans*-position.

4 Model systems for stability analyses

In this section, we elucidate the potential electronic effect of the *trans*-ligand in greater detail. For this purpose we calculated potential energy curves for N_2 coordination to model complexes **2**, with thioether and thiolate functional groups in the chelate ligand as in **1** but with the aliphatic amine bridge replaced by two methyl groups and one ligand L′ (compare Fig. 5), which may be chosen out of the spectrochemical series in order to screen different ligand field strengths in *trans*-position. We chose for our study L′ = CO (**2a**), F^- (**2b**), H_2O (**2c**), NH_3 (**2d**), H_2S (**2e**), and a complex **3**, which has been derived from **1** by replacing the amine -NH- moiety in the aliphatic chain by an ether functional group -O-.

All potential energy curves for the coordination of N_2 at these complexes are depicted in Fig. 6. The inlay structures in these diagrams also contain the structural parameters (bond lengths) of these molecules. Complexes **2b–e** and **3** possess a singlet six-coordinate minimum structure, in which N_2 is bound to the model complexes. The coordination energies on the singlet potential energy surface are about −60 kJ/mol for **2b,c** and **3** and a bit smaller for **2d** and **2e** (all values are given in column 3 in Table 1). Table 1 also contains the true coordination energy, which takes the structural relaxation and spin state change of the metal fragment into account (column 5 in Table 1). Complex **2a** with the strong *trans*-ligand L′ = CO is an exceptional case as the singlet curve is repulsive (compare also the negligible electronic binding energy of −0.2 kJ/mol given in Table 1; a zero-point vibrational energy

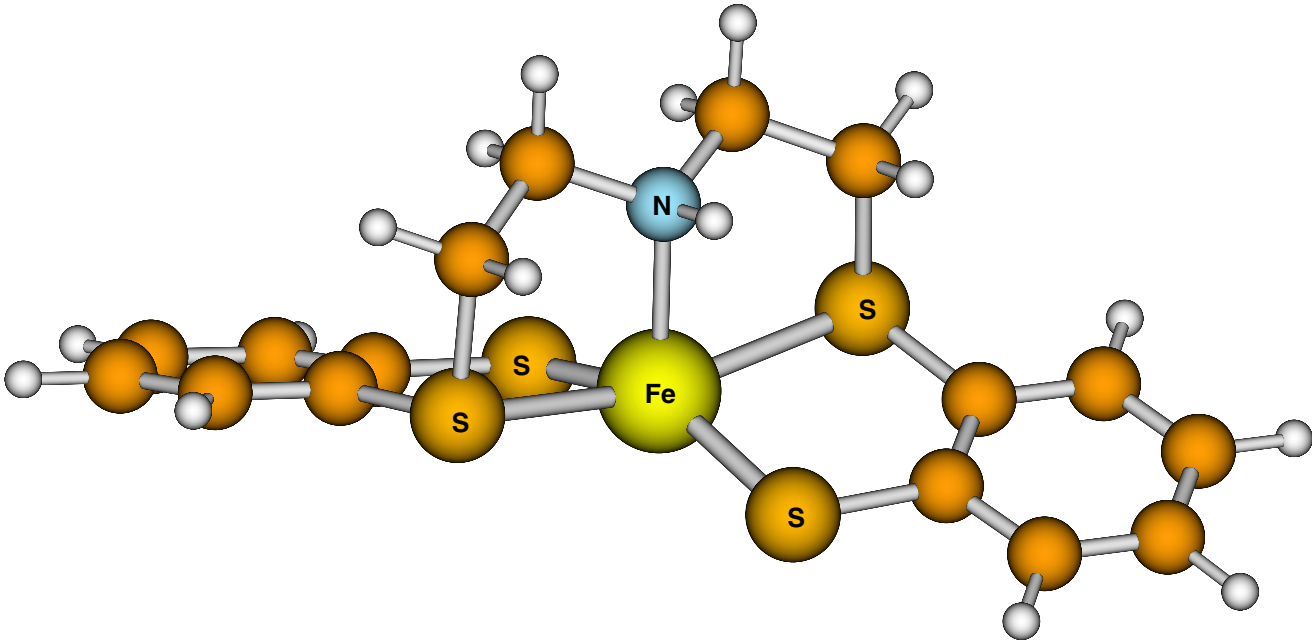

Fig. 4 Optimized high-spin quintet structure of the trigonal-bipyramidally distorted metal fragment of complex **1**

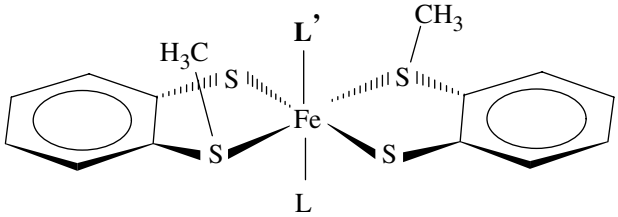

Fig. 5 Lewis structure of model compounds **2** for the study of the *trans* effect

correction, which would lead to N_2 repellance, has not been included).

We note that the intermediate spin state always lies between high- and low-spin states for these model systems as in the case of complex **1**. They have therefore been omitted for the sake of brevity. Moreover, we should emphasize that the relaxed high-spin metal fragments of the model complexes **2a–e** and **3**, whose energies are given relative to the six-coordinate minimum structures as a black bar on the right-hand-side of each diagram in Fig. 6, all adopt a trigonal-bipyramidal distorted structure of the type depicted in Fig. 4.

From the coordination energies on the singlet potential energy surface, we may conclude that coordination of N_2 is energetically favorable, especially if weak ligands like F^-, NH_3, or H_2O are in *trans*-position. Even if a chelate ligand keeps the *trans*-donor atom at distance (compare **1** with **2d**, where the Fe–N(*trans*) distance is about 3 pm larger in the bridged chelate ligand, and **3** with **2c**, where the Fe–O(*trans*) distance is about 4 pm larger in the bridged chelate ligand), the coordination energy is little affected.

As in the case of **1** discussed in the last section, the low-lying quintet state quenches the coordination energy of N_2 on the singlet potential energy curve and leads in all cases to an endothermic coordination energy (column 5 in Table 1). However, the quintet energies calculated as vertical excitations at the fixed singlet structures are almost all exothermic (column 4 in Table 1) and indicate that it is the structural relaxation of the metal fragment, which has to be inhibited through a suitably chosen chelate ligand. Such a chelate ligand should freeze a square-pyramidal structure so that it cannot rearrange to become trigonal-bipyramidal. Moreover, the diagrams in Fig. 6 cleary show that the quintet state for such a frozen square-pyramidal structure can be pushed away from the singlet state to higher energies the stronger the ligand in *trans*-position is. In particular, the potential energy curves for vertical excitation into the quintet state lie sufficiently above the singlet states for the amine and ammine complexes **1** and

Table 1 Coordination energies for various iron–sulfur complexes in different electronic states. In all cases, the reference energy is taken as the energy of the singlet minimum structure minus the energy of an isolated N_2 molecule. ΔE_A denotes its difference to the singlet metal fragment, ΔE_B denotes its difference to the quintet metal fragment calculated at the singlet asymptotic structure, and ΔE_C denotes its difference to the relaxed quintet metal fragment in kJ/mol. The $\star$ marks an energy that was obtained for the fully optimized complex **2a**, which was found to be a little lower in energy than the minimum depicted in Fig. 6, where the Fe–N bond distance was kept fixed as a constraint. The effect of this constraint was by far less pronounced for all other structures

Complex	L′	ΔE_A	ΔE_B	ΔE_C
1		−56.1	−79.7	1.8
2a	CO	−0.2*	−156.2	−32.9
2b	F^-	−59.4	1.9	81.6
2c	H_2O	−59.4	−38.5	25.4
2d	NH_3	−41.6	−52.4	20.7
2e	H_2S	−29.5	−57.5	28.6
3		−60.7	−39.4	30.6

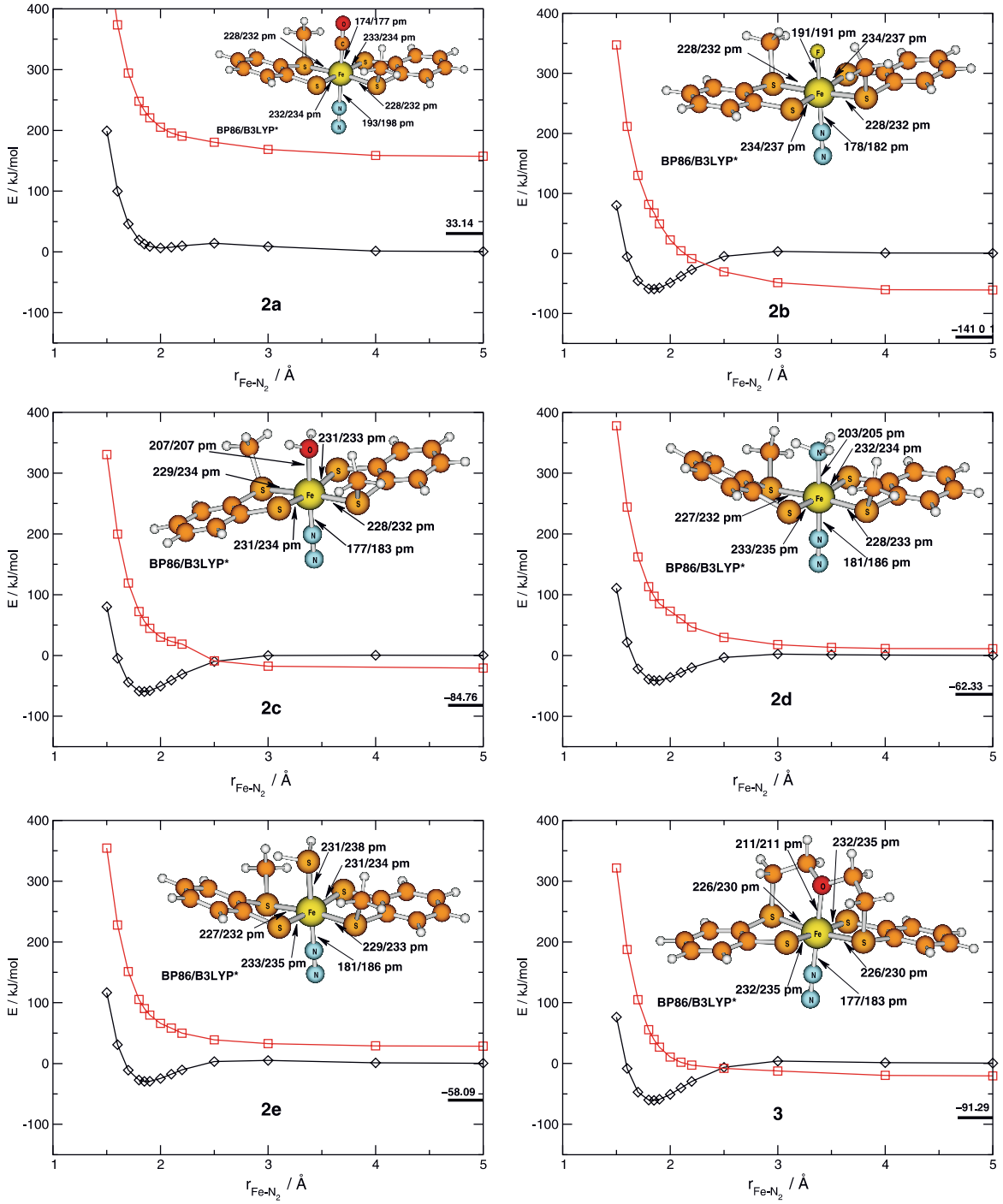

Fig. 6 Counterpoise-corrected potential energy curves (B3LYP*/TZVP) for *trans*-effect model compounds **2a–e** and **3**. *Red curve*: quintet state, *black curve*: singlet state. Bond distances of the optimized singlet minimum structure are given for BP86/RI/TZVP and B3LYP*/TZVP

2d, respectively, suggesting that nitrogen donor atoms are appropriate donors in combination with thiolate and thioether functionalities if a rigid square-pyramidal chelate ligand can be designed for these complexes.

Finally, we should make a short comment on N_2 activation in the six-coordinate singlet structures. In order to analyze the activation of the N≡N ligand, we carried out population analyses, whose results are given in Table 2 in combination with the corresponding N≡N bond distances. The PABOON partial charges indicate a small polarization of the N_2 moiety by the metal fragment, which is essentially the same in all metal complexes studied. The bond distances are about 113 pm in all complexes if calculated with BP86/RI/TZVP (and about 111 pm in B3LYP*/TZVP calcu-

Table 2 PABOON partial charges for the metal center in the six-coordinate complexes (third column) and in the five-coordinate metal fragments (sixth column) and for the nitrogen atoms coordinated to the iron center (N1) and for those (N2), which are bound to N1. The last column contains the N≡N bond distances r_{NN} in pm for BP86/RI/TZVP (and for B3LYP*/TZVP in parentheses)

Complex	L′	q(Fe)	q(N1)	q(N2)	q(Fe[fragment])	r_{NN}
1		0.2064	0.3622	0.0530	−0.6863	113 (111)
2a	CO	−0.3567	0.2825	0.1644	0.5744	111 (112)
2b	F^-	0.5159	0.3613	0.0273	0.6591	113 (111)
2c	H_2O	0.2731	0.4228	0.1056	0.8583	113 (111)
2d	NH_3	0.3583	0.3910	0.0687	−0.4469	113 (111)
2e	H_2S	−0.2389	0.4050	0.0832	−0.6818	112 (111)
3		−0.4425	0.4423	0.0728	−0.8491	113 (111)

lations). This is close to 110 pm, which we obtained for the isolated N_2 molecule (with both density functionals using a TZVP basis set).

Our results show that the inert dinitrogen molecule can be bound to Sellmann-type complexes but does not experience a significant activation in such a way that reduction to diazene is facilitated. This has already been observed in previous studies [15, 16], where we suggested an alternative electronic activation mechanism, which does not require any significant direct activation of N_2 upon coordination.

5 Conclusion

In this work, we tried to answer the question why it has not yet been possible to synthesize a dinitrogen iron(II) complex in a sulfur ligand sphere, which would be an essential step in biomimetic nitrogen fixation at iron–sulfur complexes. For Sellmann-type metal complexes we find that coordination of N_2 is in principle energetically favorable if the coordination reaction takes place on the singlet potential energy surface. Dissociation of the N_2 ligand turns out to be thermodynamically favorable because of a significant energy gain upon intersystem crossing and structural relaxation of the resulting high-spin five-coordinate metal fragment. Vertical excitation energies obtained for a series of model complexes show that this 'side reaction' could be suppressed if a square-pyramidal chelate ligand can be designed.

Acknowledgements Financial support by the Collaborative Research Centre SFB 583 "Redoxaktive Metallkomplexe", by the German science foundation DFG (Re 1703/A) and by the Fonds der Chemischen Industrie are gratefully acknowledged.

References

1. Leigh GJ (ed) (2002) Nitrogen fixation at the millenium. Elsevier, Amsterdam
2. Sellmann D, Sutter J (1996) J Biolog Inorg Chem 1:587–593
3. Sellmann D, Sutter J (1997) Acc Chem Res 30:460–469
4. Sellmann D, Sutter J (2000) Biological N_2 fixation: molecular mechanism of the nitrogenase catalyzed N_2 dependent HD-formation, the N_2 fixation inhibition and the open-side FeMoco model. In: Trzeciak AM, Sobota D, Ziolkowski J (eds) Perspectives in coordination chemistry, vol. 5. University of Wroclaw, Poland
5. Sellmann D, Utz J, Blum N, Heinemann FW (1999) Coord Chem Rev 190–192:607–627
6. Yandulov DV, Schrock RR (2003) Science 301:76–78
7. Schrock RR (2003) Chem Comm 19:2389–2391
8. Leigh GJ (2003) Science 301:55–56
9. Einsle O, Tezcan FA, Andrade SLA, Schmid B, Yoshida M, Howard JB, Rees DC (2002) Science 297:1696–1700
10. Dance I (2003) Chem Comm 3:324–325
11. Hinnemann B, Nørskov JK (2003) J Am Chem Soc 125:1466–1467
12. Schimpl J, Petrilli HM, Blöchl PE (2003) J Am Chem Soc 125:15772–15778
13. Hinnemann B, Nørskov JK (2004) J Am Chem Soc 126:3920–3927
14. Reiher M, Hess BA (2004) Adv Inorg Chem 56:55–100
15. Reiher M, Kirchner B, Hutter J, Sellmann D, Hess BA (2004) Chem Eur J 10:4443–4453
16. Kirchner B, Reiher M, Hille A, Hutter J, Hess BA (2004) Chem Eur J (in press)
17. Sellmann D, Hautsch B, Rösler A, Heinemann FW (2001) Angew Chem 113:1553–1558
18. Sellmann D, Hautsch B, Rösler A, Heinemann FW (2001) Angew Chem Int Ed 40:1505–1507
19. Sellmann D, Hille A, Heinemann FW, Moll M, Brehm G, Reiher M, Hess BA, Schneider S (2003) Inorg Chim Acta 348:194–198
20. Sellmann D, Hille A, Rösler A, Heinemann FW, Moll M, Brehm G, Schneider S, Reiher M, Hess BA, Bauer W (2003) Chem Eur J 10:819–830
21. Reiher M, Hess BA (2002) Chem Eur J 8:5332–5339
22. Deng L, Margl P, Ziegler T (1999) J Am Chem Soc 121:6479–6487
23. Ghosh A, Vangberg T, Gonzalez E, Taylor P (2001) J Porph Phthalocyan 5:345–356
24. Paulsen H, Duelund L, Winkler H, Toftlund H, Trautwein AX (2001) Inorg Chem 40:2201–2203
25. Reiher M, Salomon O, Hess BA (2001) Theor Chem Acc 107:48–55
26. Reiher M, Salomon O, Sellmann D, Hess BA (2001) Chem Eur J 7:5195–5202
27. Becke AD (1993) J Chem Phys 98:5648–5652
28. Stephens PJ, Devlin FJ, Chabalowski CF, Frisch MJ (1994) J Phys Chem 98:11623–11627
29. Reiher M (2002) Inorg Chem 41:6928–6935
30. Salomon O, Reiher M, Hess BA (2002) J Chem Phys 117:4729–4737
31. Franke O, Wiesler BE, Lehnert N, Näther C, Ksenofontov V, Neuhausen J, Tuczek F (2002) Inorg Chem 41:3491–3499
32. Keogh DW, Poli R (1997) J Am Chem Soc 119:2516–2523
33. Becke AD (1988) Phys Rev A 38: 3098-3100
34. Perdew JP (1986) Phys Rev B 33:8822–8824
35. Koch W, Holthausen MC (2000) A chemist's guide to density functional theory. Wiley-VCH, Weinheim
36. Ahlrichs R, Bär M, Häser M, Horn H, Kölmel C (1989) Chem Phys Lett 162:165–169
37. Eichkorn K, Treutler O, Öhm H, Häser M, Ahlrichs R (1995) Chem Phys Lett 240:283–290
38. Eichkorn K, Weigend F, Treutler O, Ahlrichs R (1997) Theor Chem Acc 97:119–124
39. Schäfer A, Huber C, Ahlrichs R (1994) J Chem Phys 100:5829
40. Neugebauer J, Reiher M, Kind C, Hess BA (2002) J Comput Chem 23:895–910

41. Davidson ER (1967) J Chem Phys 46:3320–3324
42. Roby KR (1974) Mol Phys 27:81–104
43. Heinzmann R, Ahlrichs R (1976) Theoret Chim Acta 42:33–45
44. Schaftenaar G, Noordik JH (2000) J Comput-Aided Mol Design 14:123–134
45. Kind C (2000) ROTCURVE — A program for the computation of reaction coordinates, University of Erlangen-Nuremberg: (unpublished)
46. Boys SF, Bernardi F (1970) Mol Phys 19:553–566
47. van Duijneveldt FB, van Duijenveldt-van de Rijdt JGCM, van Lenthe JH (1994) Chem Rev 94:1873
48. Sellmann D, Soglowek W, Knoch F, Moll M (1989) Angew Chem 101:1244–1245
49. Sellmann D, Soglowek W, Knoch F, Moll M (1989) Angew Chem 28:1271–1272